CP-violating phase on magnetized toroidal orbifolds

Tatsuo Kobayashi,[a] **Kenji Nishiwaki**[b,1] **and Yoshiyuki Tatsuta**[c]

[a]*Department of Physics, Hokkaido University,*
Sapporo 060-0810, Japan

[b]*School of Physics, Korea Institute for Advanced Study,*
Seoul 02455, Republic of Korea

[c]*Department of Physics, Waseda University,*
Tokyo 169-8555, Japan

E-mail: kobayashi@particle.sci.hokudai.ac.jp, nishiken@kias.re.kr,
y_tatsuta@akane.waseda.jp

ABSTRACT: We study the CP-violating phase of the quark sector on T^2/Z_N ($N = 2, 3, 4, 6$) with non-vanishing magnetic fluxes, where properties of possible origins of the CP violation are investigated minutely. In this system, a non-vanishing value is mandatory in the real part of the complex modulus parameter τ of the two-dimensional torus in order to explain the CP violation in the quark sector. On T^2 without orbifolding, underlying discrete flavor symmetries severely restrict the form of Yukawa couplings and it is very difficult to reproduce the observed pattern in the quark sector including the CP-violating phase $\delta_{\rm CP}$. When multiple Higgs doublets emerge on T^2/Z_2, the mass matrices of the zero-mode fermions can be written in the Gaussian textures by choosing appropriate configurations of vacuum expectation values of the Higgs fields. When such Gaussian textures of mass matrices are realized, we show that all of the quark profiles, which are mass hierarchies among the quarks, quark mixing angles, and $\delta_{\rm CP}$ can be simultaneously realized.

---

[1]Corresponding author.

Contents

1 Introduction

The standard model (SM) of particle physics had been completed by the discovery of the Higgs boson [1, 2], and it is known that the SM is a quite successful theory which can explain almost all the phenomena around the electroweak scale with great accuracy. However, since we know that some theoretical difficulties prevail in the SM, various phenomenological models beyond the SM of particle physics have been proposed and investigated steadily.

Addressing extra dimensions is known to be an avenue to distinctive phenomenological model buildings. Indeed, several models can solve phenomenological problems, e.g., the gauge hierarchy problem [3–5], doublet-triplet splitting problem in supersymmetric SU(5) grand unified theory (GUT) [6, 7], tiny neutrino masses [8], the flavor puzzle among the SM quarks and leptons [9, 10] and so on. On the other hand, superstring theories predict the existence of extra six dimensions (6D) due to their theoretical consistency, i.e., the totally ten dimensions (10D) are involved. Phenomenologies inspired by superstring theory have been enthusiastically studied from the late 1980's. Thus, from both of phenomenological bottom-up and theoretical top-down points of view, models on extra dimensions play an important role in concrete model building.

Recently, higher dimensional supersymmetric Yang-Mills (SYM) theories compactified on two-dimensional (2D) torus T^2, or toroidal orbifolds T^2/Z_N ($N = 2, 3, 4, 6$), as well as 6D torus and orbifolds have attracted much attentions. Obviously, six-dimensional models have larger degrees of freedom in boundary conditions than five-dimensional models. On top of that, higher dimensional gauge theories such as the SYM theory are more interesting since we can put non-vanishing magnetic fluxes, which are vacuum expectation values of extra-dimensional components of a higher dimensional vector field. Indeed, such higher dimensional SYM theories with non-vanishing magnetic fluxes are often used in the context of higher dimensional (supersymmetric) GUTs. It is attractive to use such magnetic

fluxes from the standpoint of theoretical and phenomenological model buildings, because the SYM theory compactified on 6D spacetime including 2D torus with magnetic fluxes can lead to several phenomenological ingredients, e.g., chiral (supermultiplet) matter fields, their generations, and (three-point) Yukawa couplings and so on [11]. Indeed, phenomenological aspects of the higher dimensional SYM theory with non-vanishing magnetic fluxes have been investigated, e.g., extensions to toroidal orbifolds [12, 13], analyses of zero-mode wavefunctions [14, 15], three-generation models [16, 17], the minimal supersymmetric standard model (MSSM) and its modified models [18, 19], non-Abelian discrete flavor symmetries [20–23], realistic flavor structures of quarks and leptons [24], and other studies [25–31].

The four-dimensional CP symmetry can be embedded into 10D Lorentz symmetry with positive determinant in 10D SYM theories and superstring theory [32, 33]. That is, we can combine the 4D CP transformation and extra 6D transformation with negative determinant to make a 10D proper Lorentz transformation. For example, when we denote the complex coordinates of the extra 6D space by z^a ($z^a \equiv y_{2a+3} + i\, y_{2a+4}$, $a = 1, 2, 3$), the 4D CP transformation with $z^a \to (z^a)^*$ is the 10D Lorentz transformation. That is a good symmetry on the trivial background.[1] We may also have other embedding, whose transformation of the extra 6D space leads to the transformation with negative determinant. However, nontrivial geometrical and gauge backgrounds violate such a CP symmetry embedded in higher dimensions and the 4D CP symmetry could be violated [36–38]. Then, CP-violating phases would appear in 4D low-energy effective field theory. For example, a certain type of orbifolds break the symmetry $z^a \to (z^a)^*$ [37, 38] and magnetic fluxes also break such a symmetry. Violation of the CP symmetry does not always lead to non-vanishing Kobayashi-Maskawa (KM) CP phase $\delta_{\rm CP}$ [39] (at tree level), although it would lead to some CP-violating terms. Obviously, Yukawa couplings should have nontrivial CP phases, which cannot be canceled by rephasing fields. In higher dimensional SYM theories, the Yukawa coupling is obtained by the product of the higher dimensional gauge coupling and overlap integral of zero-mode wavefunctions in the compact space. Thus, the wavefuncitons and its overlap integral must be nontrivial to realize the physical CP phase. The constant zero-mode profiles on the simple torus and oribifold could not lead to non-vanishing physical CP phase within the framework of pure SYM theories. Also, the coupling selection rule as well as the flavor symmetry would be important to realize non-vanishing mixing and KM phase [37].

In this paper, we study KM CP-violating phase within the framework of 10D SYM theories on magnetized orbifolds. Zero-mode profiles on the torus and orbifolds are quite nontrivial, and their couplings include nontrivial phases. The models on the torus with magnetic flux has a large symmetry [20] and orbifolding would be helpful to violate such a symmetry and to realize non-vanishing physical CP phase.

We study the CP-violating phase of the quark sector on T^2/Z_N ($N = 2, 3, 4, 6$) with non-vanishing magnetic fluxes. In the case of multiple Higgs doublets emerging, the mass matrices of the zero-mode fermions can be written in the Gaussian texture by choosing appropriate configurations of vacuum expectation values of the Higgs fields [24]. When such Gaussian textures of mass matrices are realized, we show that all of the quark profiles, which

---

[1]That provides a solution of the strong CP problem [34, 35].

are mass hierarchies among the quarks, quark mixing angles including the CP-violating phase δ_{CP}, can be simultaneously realized.

This paper is organized as follows. In section 2, we briefly review Yukawa couplings and mass matrices on magnetized orbifolds T^2/Z_N ($N = 2, 3, 4, 6$). Then, we focus on the quark sector of the SM and identify the Yukawa couplings and the mass matrices with those of the quarks. In section 3, we study what is important to realize non-vanishing δ_{CP} in simple examples. In section 4, we introduce our strategy of analyzing the CP-violating phase δ_{CP} in the quark sector and show results of numerical calculations with mentioning possible origins of the CP-violating phase in the quark sector on magnetized toroidal orbifolds T^2/Z_N. Section 5 is devoted to conclusions and discussions. In appendix A, we provide additional examples of numerical calculations under different setups on magnetized orbifolds.

2 Quark mass matrix on magnetized T^2/Z_N

In this section, we briefly review the form of the mass matrices on toroidal orbifolds T^2/Z_N ($N = 2, 3, 4$ and 6) with magnetic fluxes in 6D spacetime, based on [17, 40]. The 2D orbifold among the 6D space is important for the flavor structure. Thus, we concentrate ourselves on the 2D orbifold part here.

First of all, we consider three sectors (labelled as "1", "2", "3") which constitute (three-point) Yukawa-type interactions. The analytical expression of the Yukawa couplings on a magnetized T^2/Z_N is given as

$$\widetilde{\lambda}'_{I',J',K'} = \sum_{I=0}^{|M_1|-1} \sum_{J=0}^{|M_2|-1} \sum_{K=0}^{|M_3|-1} \lambda_{I,J,K} \left(\mathcal{U}^{Z_N;\eta_1}\right)_{I,I'} \left(\mathcal{U}^{Z_N;\eta_2}\right)_{J,J'} \left(\mathcal{U}^{Z_N;\eta_3}\right)^*_{K,K'}, \quad (2.1)$$

where $\lambda_{I,J,K}$ represents the Yukawa couplings on a magnetized T^2,

$$\lambda_{I,J,K} = \sum_{m \in Z_{M_3}} \delta_{I+\alpha_1+J+\alpha_2+mM_1,\, K+\alpha_3+\ell M_3} \times \vartheta \begin{bmatrix} \frac{M_2(I+\alpha_1)-M_1(J+\alpha_2)+mM_1M_2}{M_1M_2M_3} \\ 0 \end{bmatrix}(X,Y), \quad (2.2)$$

$$X := M_1\beta_2 - M_2\beta_1, \qquad Y := M_1M_2M_3\tau, \quad (2.3)$$

where I, J, K identify the degenerated states on the magnetized torus of the sectors "1", "2", "3", respectively. In the low energy effective theory, zero-modes of the X-th matter fields ($X = 1, 2, 3$) are characterized by the magnitudes of magnetic fluxes M_X, Scherk-Schwarz (SS) phases α_X and β_X, and Z_N parities η_X, respectively. We note that this form is for the case of $M_{1,2,3} > 0$. Here, the consistency conditions are held:

$$M_1 + M_2 = M_3, \quad \alpha_1 + \alpha_2 = \alpha_3, \quad \beta_1 + \beta_2 = \beta_3, \quad \eta_1\eta_2(\eta_3)^\dagger = 1. \quad (2.4)$$

The complex structure modulus parameter of the torus is designated by τ. Here, we ignored an overall factor, which is a function of $M_{1,2,3}$. I', J' and K' label the (physical) flavor eigenstates of the three kinds of matter fields appearing the Yukawa interaction, where the kinetic terms of the zero-modes are suitably diagonalized, whereas the Yukawa coupling matrix is not yet diagonalized. The index I' (J', K') runs from 0 to rank $[\mathcal{K}^{(Z_N;\eta_1)}]$ –

1 (rank $[\mathcal{K}^{(Z_N;\eta_2)}]-1$, rank $[\mathcal{K}^{(Z_N;\eta_3)}]-1$), respectively. ϑ denotes the Jacobi's theta function whose definition is given as

$$\vartheta \begin{bmatrix} a \\ b \end{bmatrix} (c\nu, c\tau) = \sum_{l=-\infty}^{\infty} e^{i\pi(a+l)^2 c\tau} e^{2\pi i(a+l)(c\nu+b)}, \tag{2.5}$$

where a and b are real numbers, c is an integer, and ν and τ are complex numbers with $\mathrm{Im}\,\tau > 0$, respectively. In eq. (2.1), it is easily found that the Yukawa couplings on T^2 are mixed by the matrices,

$$(\mathcal{U}^{Z_N;\eta_X})_{\mathcal{I},\mathcal{I}'} = \sum_{\mathcal{I}''=0}^{|M_X|-1} (\mathcal{K}^{(Z_N;\eta_X)})_{\mathcal{I},\mathcal{I}''}(U^{(Z_N;\eta_X)})_{\mathcal{I}'',\mathcal{I}'}, \tag{2.6}$$

where $\mathcal{K}^{(Z_N;\eta_X)}$ and $U^{(Z_N;\eta_X)}$ describe the effects via the projection from T^2 onto T^2/Z_N and the diagonalization of the kinetic terms of the sector X, respectively. Concrete forms of $\mathcal{K}^{(Z_N;\eta_X)}$ and $U^{(Z_N;\eta_X)}$ are provided in ref. [40]. In the following part, we identify the first matter fields in the sector "1" with left-handed quarks, the second ones in the sector "2" with right-handed quarks and the third ones in the sector "3" with Higgs doublet fields. Also, we require three generations in the left-handed and right-handed quarks. Thus, in the following, we assume the primed indices among the left-handed and right-handed quarks run over $I', J' = 0, 1, 2$. We note that possibilities to realize such three-generation models were investigated in ref. [14].[2]

In a case with n_H generations in the Higgs fields, i.e., $K' = 0, 1, \ldots, n_H - 1$, the quark mass matrix consists of the Yukawa couplings in eq. (2.1) and the Higgs vacuum expectation values (VEVs) ($v_{K'}$) as

$$M_{I',J'} = \sum_{K'=0}^{n_H-1} \widetilde{\lambda}'_{I',J',K'} \times v_{K'}. \tag{2.7}$$

In this paper, we do not construct complete models where all of ten-dimensional (10D) configurations are manifested (not only the flavor part of the quark and Higgs sectors). We respect a procedure of classifying possible configurations of the quark sector in ref. [24], and consider the case of multiple up- and down-type Higgs doublets emerging as,

$$(M_u)_{I',J'} = \sum_{K'=0}^{n_H-1} \widetilde{\lambda}'_{I',J',K'} \times v_{uK'}, \tag{2.8}$$

$$(M_d)_{I',J'} = \sum_{K'=0}^{n_H-1} \widetilde{\lambda}'_{I',J',K'} \times v_{dK'}, \tag{2.9}$$

where $v_{uK'}$ ($v_{dK'}$) are VEVs of up-type (down-type) Higgs fields in the MSSM-like Higgs sector, respectively. In the next section, we analyze the above type of mass matrices in order to investigate the CP-violating phase in the quark sector.

----

[2]See also ref. [17].

3 Basic properties of a CP-violating phase

In this section, we survey basic properties of the CP-violating phase originating from the quark Yukawa couplings of the magnetized orbifold model, where the model is expected to be derived from the 10D supersymmetric Yang-Mills theory which is a low-energy effective theory of superstring theories. As widely known, observing complex degrees of freedom in the Yukawa couplings (in flavor eigenstates) is a necessary condition for realizing a CP-violating phase (in quark mass eigenstates) [39].

Extra-spacial components of a 10D vector field behave as scalars from the four-dimensional point of view, which can be candidates of (multiple) Higgs bosons. Here, no complex parameter exists in the 10D action, but this is not the end of the story. A CP-violating phase can be realized in the following reason. On the magnetized T^2, the mode function with the flavor index I of the matter field X which feels the magnetized flux M_X (> 0) and SS phases (α_X, β_X) is given as the following form

$$\Theta_{M_X}^{(I+\alpha_X,\beta_X)}(z,\tau) \propto e^{i\pi M_X z \frac{\mathrm{Im}(z)}{\mathrm{Im}\tau}} \cdot \vartheta \begin{bmatrix} \frac{I+\alpha_X}{M_X} \\ -\beta_X \end{bmatrix} (M_X z, M_X \tau), \tag{3.1}$$

where an overall factor is not important in the following discussions and is neglected.[3] As discussed in refs. [36–38] and we touched in Introduction, in even spacetime dimensions, under the "modified" CP transformation, which corresponds to the ordinary "4D" CP transformation after the Kaluza-Klein decomposition, the complex coordinate z is transformed as the complex conjugation; "4D" CP: $z \to z^*$ [36–38]. The zero-mode function in eq. (3.1) is not invariant under the transformation, which is ensured by the non-zeroness of the following variables; $\mathrm{Re}\,\tau$, M_X, α_X and/or β_X. Then in general, effective Yukawa couplings can be complex and the above necessary condition is fulfilled.

On the other hand, the existence of the complex degrees of freedom itself is not a sufficient condition for the emergence of a CP-violating phase. In the present model, Yukawa couplings cannot take arbitrary components, the values of which are determined by the fundamental parameters; τ, M_X, α_X and β_X. Then, if the structure of the up- and down-type quark sectors are similar, the degree of freedom of a complex phase is expected to vanish because the Cabbibo-Kobayashi-Maskawa (CKM) matrix V_{CKM} [39] is defined by use of the diagonalizing matrices for the sectors of the up-type quarks (U_u) and down-type ones (U_d),

$$V_{\mathrm{CKM}} \equiv U_u(U_d)^\dagger, \tag{3.2}$$

whose physical components are usually parametrized as

$$V = V_{\mathrm{CKM}} = \begin{pmatrix} c_{12}c_{13} & s_{12}c_{13} & s_{13}e^{-i\delta_{\mathrm{CP}}} \\ -s_{12}c_{23} - c_{12}s_{23}s_{13}e^{i\delta_{\mathrm{CP}}} & c_{12}c_{23} - s_{12}s_{23}s_{13}e^{i\delta_{\mathrm{CP}}} & s_{23}c_{13} \\ s_{12}s_{23} - c_{12}c_{23}s_{13}e^{i\delta_{\mathrm{CP}}} & -c_{12}s_{23} - s_{12}c_{23}s_{13}e^{i\delta_{\mathrm{CP}}} & c_{23}s_{13} \end{pmatrix}. \tag{3.3}$$

It is noted that if the structures of the up- and down-type quarks are completely the same, the relation $U_u = U_d$ results in the trivial mixing $V_{\mathrm{CKM}} \to \mathbf{1}_3$.

---

[3]When $M_X < 0$, the anti-holomorphic counterpart ($z \to \bar{z}$, $\tau \to \bar{\tau}$) comes in the mode function.

In the following part, we show illustrating samples for the non-vanishing CP violation where the realization of the flavor structures, e.g., the quark mass hierarchies and mixing angles are not seriously considered at this stage. We focus on the value of the CP-violating phase $\delta_{\rm CP}$. By showing such illustrating samples, we try to exemplify several origins of the CP-violating phases on magnetized orbifolds. Before going to realizations of realistic flavor structures, it would be very important to become familiar with basic characteristics of the CP violation in this system. For our purpose, we utilize the Jarlskog invariant $J_{\rm CP}$ [41, 42], which is defined as

$$J_{\rm CP} = \text{Im}\,[V_{12}V_{22}V_{12}^*V_{21}^*]. \tag{3.4}$$

It is invariant under field rephasing operations, and then a nonzero $J_{\rm CP}$ indicates the existence of a nonzero CP-violating phase $\delta_{\rm CP}$.

To declare the structure of the CP violation carefully, let us consider cases with one up-type Higgs and one down-type Higgs ($n_H = 1$). At first, we comment on the configurations on T^2 without orbifolding to compare it with the following orbifold models. Here, the magnitudes of the magnetic fluxes are uniquely fixed for realizing three generations in the quarks as $M_1 (= M_{1'}) = -3$, $M_2 (= M_{2'}) = -3$, $M_3 (= M_{3'}) = +6$, where six pairs of up- and down-type Higgs boson doublets emerge. In the following discussion, for clarity, we adopt the notation on variables as $M_1 + M_2 + M_3 = 0$, $\alpha_1 + \alpha_2 + \alpha_3 = 0$, $\beta_1 + \beta_2 + \beta_3 = 0$, $\eta_1\eta_2\eta_3 = 1$, which are different from those in eq. (2.4).

Unfortunately on the simplest geometry, Yukawa couplings in eq. (2.2) obey discrete flavor symmetries and major parts of the matrix elements are forced to be zero. On the present magnetic fluxes, the hidden symmetry becomes $\Delta(27)$ [20] and only the diagonal form and permuted ones of it are possible in the three-by-three Yukawa matrix of eq. (2.2) with a fixed K (now, $K = 0, 1, 2, 3, 4, 5$). Thereby, at least in the case that only one up-type Higgs and one down-type Higgs contain nonzero VEVs, there exists at least one vanishing mixing angle inevitably, and eventually and manifestly $J_{\rm CP}$ becomes zero.[4] Then, to violate the discrete flavor symmetry would be required for (quasi-)realistic models. A possible way of breaking the symmetry is to introduce orbifolding. As we concretely look in the subsequent discussion, even under the simplest Z_2 case, such a discrete symmetry is violated and nonzero $J_{\rm CP}$ gets to be achievable.

Next, we move to the configurations shown in table 1, where we fix the parameters for the left-handed quarks. In Sample I, the up-type and down-type mass matrices of the quarks originate from the same magnetic fluxes and SS twist phases. In comparison with Sample I and II, we can find whether the difference of the SS twists could be important for the CP violation or not. Similarly, in comparison with Sample I and III, we can investigate the importance of the different fluxes in the up-type and down-type quarks. In Sample IV, we consider the different magnetic fluxes and SS twist phases. In the following part of this section, we set $\text{Re}\,\tau \in [-\pi, \pi]$ and $\text{Im}\,\tau = 1$, for simplicity.

---

[4]In ref. [37], it was found that the coupling selection rules are quite strong and we cannot realize non-vanishing CP phase in certain heterotic orbifold models, although Yukawa couplings in general have nontrivial CP phases.

	left-handed quarks $\{M_1, \alpha_1, \beta_1, \eta_1\}$	right-handed up-types $\{M_2, \alpha_2, \beta_2, \eta_2\}$ right-handed down-types $\{M_{2'}, \alpha_{2'}, \beta_{2'}, \eta_{2'}\}$	up-type Higgs doublet $\{M_3, \alpha_3, \beta_3, \eta_3\}$ down-type Higgs doublet $\{M_{3'}, \alpha_{3'}, \beta_{3'}, \eta_{3'}\}$
Sample I	$\{-5, 0, 0, +1\}$	$\{+6, 0, \frac{1}{2}, +1\}$ $\{+6, 0, \frac{1}{2}, +1\}$	$\{-1, 0, \frac{1}{2}, +1\}$ $\{-1, 0, \frac{1}{2}, +1\}$
Sample II	$\{-5, 0, 0, +1\}$	$\{+6, 0, \frac{1}{2}, +1\}$ $\{+6, \frac{1}{2}, \frac{1}{2}, -1\}$	$\{-1, 0, \frac{1}{2}, +1\}$ $\{-1, \frac{1}{2}, \frac{1}{2}, -1\}$
Sample III	$\{-5, 0, 0, +1\}$	$\{+6, 0, \frac{1}{2}, +1\}$ $\{+7, 0, \frac{1}{2}, -1\}$	$\{-1, 0, \frac{1}{2}, +1\}$ $\{-2, 0, \frac{1}{2}, -1\}$
Sample IV	$\{-5, 0, 0, +1\}$	$\{+6, 0, \frac{1}{2}, +1\}$ $\{+7, \frac{1}{2}, \frac{1}{2}, +1\}$	$\{-1, 0, \frac{1}{2}, +1\}$ $\{-2, \frac{1}{2}, \frac{1}{2}, +1\}$

Table 1. Sample patterns in proving an origin of the CP violation.

At first, we comment on Sample I. In Sample I, it is obviously found that the CKM matrix is the unit matrix (irrespective of the value of τ) because the mass matrices of the up- and down-sectors are equivalent. Then, the Jarlskog invariant $J_{\rm CP}$ becomes zero, and the CP symmetry still remains in the mass matrices at this level. The important lesson from this example is that at least either of the magnetic fluxes or the pairs of the SS phases should be different for realizing a nonzero $\delta_{\rm CP}$.
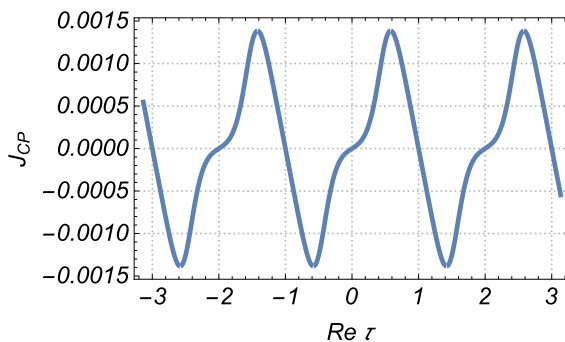
Figures 1, 2, 3 show the relationships between the real part of the complex structure modulus $\mathrm{Re}\,\tau$ and the Jarlskog invariant $J_{\rm CP}$ in the cases of II, III, IV, respectively. Figure 1 tells us that the non-integer values of $\mathrm{Re}\,\tau$ ($\mathrm{Re}\,\tau \notin \mathbb{Z}$) break the CP symmetry. In particular, it should be noted that the vanishing $\mathrm{Re}\,\tau$ ($\mathrm{Re}\,\tau = 0$) preserve the CP in the mass matrices at the tree level, as we will see also in the other samples. Figures 2 and 3 suggest us that the vanishing $\mathrm{Re}\,\tau$ ($\mathrm{Re}\,\tau = 0$) does not lead to the CP breaking. Now, the following statement is confirmed: it is impossible to violate the CP without non-vanishing $\mathrm{Re}\,\tau$ in the present system.[5]

In addition, it is interesting to comment on periodic properties of $\mathrm{Re}\,\tau$ in $J_{\rm CP}$ shown in figures 1, 2 and 3. When different patterns on SS phases are imposed in the two types of quarks, the period of $\mathrm{Re}\,\tau$ becomes greater than one. Also, figure 3 would imply that $J_{\rm CP}$ can be amplified when differences are found both in magnetic fluxes and SS phases. By summarizing the results of the four illustrating samples, we can conclude that the non-vanishing $\mathrm{Re}\,\tau$ leads to the CP violation, and the observed values in $J_{\rm CP}$ ($\sim 10^{-5}$) would be realized by choosing the magnitude of $\mathrm{Re}\,\tau$, magnetic fluxes and the SS twist phases suitably.

Finally, let us emphasize that all the observed properties are in the case with one Higgs pair ($n_H = 1$). As described in eqs. (2.8) and (2.9), when multiple Higgs pairs are imposed

---

[5]In ref. [43], it was discussed that only the discrete Wilson lines, i.e., SS phases cannot lead to non-vanishing CP phase in heterotic orbifold models.
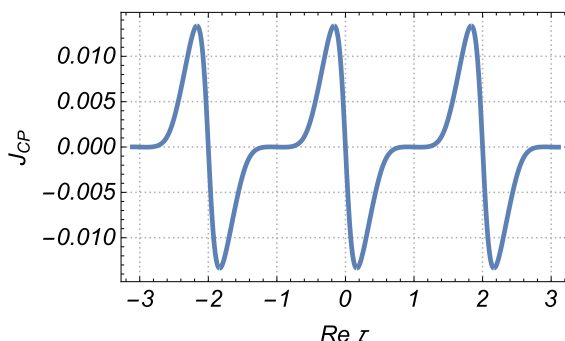
Figure 1. The relationship between a real part of the complex structure modulus $\mathrm{Re}\,\tau$ and the Jarlskog invariant J_{CP} in Sample II.
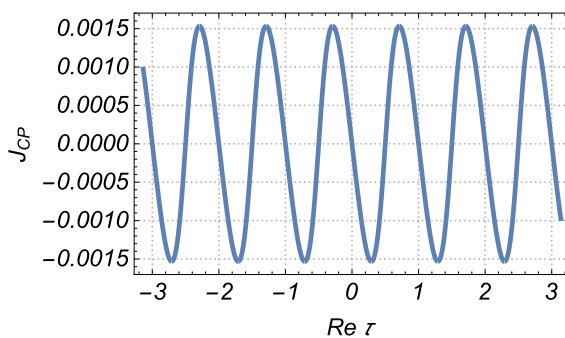
Figure 2. The relationship between a real part of the complex structure modulus $\mathrm{Re}\,\tau$ and the Jarlskog invariant J_{CP} in Sample III.

Figure 3. The relationship between a real part of the complex structure modulus $\mathrm{Re}\,\tau$ and the Jarlskog invariant J_{CP} in Sample IV.

($n_H \geq 2$), resultant Yukawa couplings become superpositions of all the contributions via the multiple Higgs boson doublets, where correspondences between $\mathrm{Re}\,\tau$ and J_{CP} would be more complicated.

We have shown that one can realize the non-vanishing CP phase in magnetized orbifold models by using simple examples. However, the above models with one pair of Higgs fields cannot completely realize realistic mass ratios and mixing angles [17, 40]. In the next section, we study numerically the models with multi-pairs of Higgs fields in order to show the possibility for realizing the quark mass ratios, mixing angles and the KM phase δ_{CP}.

4 Numerical analyses in Gaussian Froggatt-Nielsen models

In this section, we numerically analyze the CP-violating phase δ_{CP} in the configuration with multiple Higgs doublet fields. When the Higgs fields are degenerated due to non-vanishing magnetic fluxes and two or three of them contain specific non-zero VEVs, the mass matrix is approximately written in the Gaussian form [24] as

$$M_{I',J'} \sim e^{c(a_{I'}+b_{J'})^2 i\tau} = e^{-c(a_{I'}+b_{J'})^2(\mathrm{Im}\,\tau - i\mathrm{Re}\,\tau)}, \tag{4.1}$$

where $a_{I'}$, $b_{J'}$ and c are symbolized factors which are determined by the magnitudes of the magnetic fluxes, the SS phases and the boundary conditions. This property of the mass matrix is called the *Gaussian Froggatt-Nielsen (FN) mechanism* [24], which is a suitable mass matrix for explaining the observed flavor patterns in the quarks and charged leptons. Here, we focus only on $N = 2$ case (T^2/Z_2), because the Gaussian FN mechanism is not beneficial in the cases of $N = 3, 4$ and 6. As pointed out in [40], the observed mass hierarchy between the top and up quarks, i.e., $m_u/m_t = \mathcal{O}(10^{-5})$ cannot be realized since nontrivial large mixings shown by $U^{(Z_N;\eta_X)}$ smear great differences originating from quasi-localized profiles of the particles due to the existence of the magnetic fluxes. Furthermore, the value of the complex modulus parameter τ is obligated to be $e^{2\pi i/N}$ for T^2/Z_N ($N = 3, 4, 6$) due to consistencies of the orbifold identifications. When the imaginary part of τ is less than or equal to one in the T^2/Z_N ($N = 3, 4, 6$) cases, the Gaussian FN texture does not generate sizable hierarchies in $\lambda_{I',J',K'}$ in eq. (2.1). Thereby, we investigate only the T^2/Z_2 case, where the complex modulus parameter can take an arbitrary value. Before showing concrete theoretical samples of quark flavor structures, we would like to comment on the moduli stabilization. On T^2/Z_2 orbifold, the complex structure modulus is not geometrically stabilized. In this paper, we assume the moduli stabilization of the complex structure modulus τ, where we regard it as a free parameter.

Based on the previous analysis [24], it is interesting to investigate a flux configuration with five Higgs pairs ($n_H = 5$),[6]

$$\begin{aligned} M_1 = -5, \quad M_2 = -7, \quad M_3 = +12, \\ \eta_1 = +1, \quad \eta_2 = -1, \quad \eta_3 = -1, \end{aligned} \tag{4.2}$$

where various patterns are possible in the SS phases α_X and β_X ($X = 1, 2, 3$). In ref. [24], only the case with trivial SS phases $(\alpha_1, \alpha_2, \alpha_3) = (0, 0, 0)$ and $(\beta_1, \beta_2, \beta_3) = (0, 0, 0)$ were analyzed, and no discussion was made on the CP-violating phase in the quark mass matrix. In this paper, we take account of additional three patterns with the SS phases as shown in table 2. Note that the difference between Pattern I, II, III, IV are found only in the values of the SS phases. In all of the cases, the values of the Higgs VEVs are randomly selected from designated domains in our parameter searches.

Here, it is important to remind what can be an origin of the CP-violating phase. In order to obtain complex values in entries of Yukawa couplings (2.2) on T^2, we need at least

---

[6]The other example is shown in appendix A.

	left-handed quarks $\{M_1, \alpha_1, \beta_1, \eta_1\}$	right-handed quarks $\{M_2, \alpha_2, \beta_2, \eta_2\}$	Higgs fields $\{M_3, \alpha_3, \beta_3, \eta_3\}$
Pattern I	$\{-5, 0, 0, +1\}$	$\{-7, 0, 0, -1\}$	$\{+12, 0, 0, -1\}$
Pattern II	$\{-5, 1/2, 0, +1\}$	$\{-7, 1/2, 0, -1\}$	$\{+12, 0, 0, -1\}$
Pattern III	$\{-5, 0, 1/2, +1\}$	$\{-7, 0, 1/2, -1\}$	$\{+12, 0, 0, -1\}$
Pattern IV	$\{-5, 1/2, 1/2, +1\}$	$\{-7, 1/2, 1/2, -1\}$	$\{+12, 0, 0, -1\}$

Table 2. Sample patterns of configurations. Note that Pattern I is exactly the same as that of the previous paper [24].

non-vanishing values in $\mathrm{Re}\,\tau$.[7] On the other hand, in order to obtain complex values in coefficient matrices in eq. (2.2) and eq. (2.6), both of α_X and β_X should be non-vanishing. This implies that we need to input a non-vanishing value of $\mathrm{Re}\,\tau$ in Pattern I. In the other patterns, it is more general to additionally turn on a non-vanishing value of $\mathrm{Re}\,\tau$ in addition to the SS phases α_X and β_X. That is, $\mathrm{Re}\,\tau$ would be required to fit an observed value of the CP-violating phase [44],

$$\delta_{\mathrm{CP}} = 1.208 \quad [\mathrm{rad}]. \tag{4.3}$$

In the following enumeration, we show numerical results of analyzing the mass matrices via Gaussian FN mechanism.

We mention input parameters and their ranges in our setups which are used to fit mass hierarchies and mixing angles among the up- and down-type quarks. In the following numerical analyses, we choose several sample values of a complex structure modulus τ in the ranges of $\mathrm{Re}\,\tau$ (from $-\pi$ to π with each $\pi/10$ steps) and $\mathrm{Im}\,\tau \in [1.5, 2.0]$, and randomly scattered values in the (up- and down-type) Higgs VEVs with multiple generations from the ranges as the shape of the ratios,

$$\rho_u \equiv \frac{v_{u4}}{v_{u1}} \in [0, 0.4], \qquad \rho_d \equiv \frac{v_{d4}}{v_{d1}} \in [0, 0.5], \qquad \rho_d' \equiv \frac{v_{d2}}{v_{d1}} \in [0, 0.01], \tag{4.4}$$

where the others are set to be zero, as taken in ref. [24]. We examine the ratios of quark mass eigenvalues (not the absolute magnitudes of them), and then to assign the ratios is enough for our purpose. In the following analyses, we also assume that the electroweak symmetry breaking is appropriately caused by a linear combination of multiple Higgs VEVs, and that other linear combinations are heavy enough. Here, the non-zero VEVs are chosen in order to obtain the Gaussian textures of mass matrices [24]. We use relatively crude cuts by the observed data [44] for the ratios of the mass hierarchies in the up-quark sector,

$$\frac{1}{3} \le \left(\frac{m_u}{m_t}\right)_{\mathrm{obs.}} \bigg/ \left(\frac{m_u}{m_t}\right)_{\mathrm{theor.}} \le 3, \qquad \frac{1}{3} \le \left(\frac{m_c}{m_t}\right)_{\mathrm{obs.}} \bigg/ \left(\frac{m_c}{m_t}\right)_{\mathrm{theor.}} \le 3, \tag{4.5}$$

---

[7]In the case of T^2/Z_2, the form of $\mathcal{K}^{(Z_2;\eta)}$ is given as

$$(\mathcal{K}^{(Z_2;\eta)})_{K,J} = \frac{1}{2}\left(\delta_{J,K} + \eta\, e^{-2\pi i \cdot \frac{2\beta}{M}(J+\alpha)}\delta_{-2\alpha-J,K}\right),$$

where M, J and K, α and β, η are corresponding magnetic flux, torus indices, SS phases, Z_2 parity, respectively [15]. $U^{(Z_2;\eta)}$ is easily evaluated as the unitary matrix which diagonalizes the above matrix $\mathcal{K}^{(Z_2;\eta)}$. We can find that the non-vanishing SS phases α and β provide a complex phase in the matrix $\mathcal{K}^{(Z_2;\eta)}$.

	Sample values	Observed values
$(m_u, m_c)/m_t$	$(1.9 \times 10^{-5}, 1.9 \times 10^{-2})$	$(1.5 \times 10^{-5}, 7.5 \times 10^{-3})$
$(m_d, m_s)/m_b$	$(6.6 \times 10^{-4}, 2.4 \times 10^{-2})$	$(1.2 \times 10^{-3}, 2.3 \times 10^{-2})$
$\sin\theta_{12}$	0.23	0.2254
$\sin\theta_{23}$	0.075	0.04207
$\sin\theta_{13}$	0.0085	0.00364
$\delta_{\rm CP}$	1.2	1.208

Table 3. Sample values of an illustrating parameter configuration in Pattern IV as an example. Observed values are also quoted from ref. [44]. Input parameters are chosen as $\mathrm{Re}\,\tau = 0.5$, $\mathrm{Im}\,\tau = 1.7$, $\rho_u = 0.26$, $\rho_d = 0.19$ and $\rho'_d = 0.012$.

also in the down-quark sector,

$$\frac{1}{3} \le \left(\frac{m_d}{m_b}\right)_{\rm obs.} \Big/ \left(\frac{m_d}{m_b}\right)_{\rm theor.} \le 3, \qquad \frac{1}{3} \le \left(\frac{m_s}{m_b}\right)_{\rm obs.} \Big/ \left(\frac{m_s}{m_b}\right)_{\rm theor.} \le 3, \qquad (4.6)$$

and also in the quark mixing angles,

$$0.20 \le \sin\theta_{12} \le 0.25, \qquad 0.01 \le \sin\theta_{23} \le 0.10. \qquad (4.7)$$

Concrete values of the observed masses and mixing angles in the quark sector are summarized in table 3 in Pattern IV as an example. Table 3 shows that the quark mass hierarchies, small mixing angles and the CP-violating phase can be almost explained simultaneously on the magnetize orbifold T^2/Z_2 up to slight deviations from the observed values especially in m_c/m_t and $\sin\theta_{13}$.

In numerical analyses, we require the three-type conditions simultaneously, which are on the mass ratios in the up-type quarks [eq. (4.5)], on the mass ratios in the down-type quarks [eq. (4.6)], and on the two of mixing angles [eq. (4.7)]. The number of trials in randomly scattering parameters is 5×10^4 for each fixed value of $(\mathrm{Re}\,\tau, \mathrm{Im}\,\tau)$. When a configuration of eq. (4.4) passes the above cuts, we calculate the corresponding value of the CP-violating phase.

Numerical analysis in Pattern I. Results are shown in figures 4 (for $\mathrm{Im}\,\tau = 1.8$) and 5 (for $\mathrm{Im}\,\tau = 2.0$), which indicate that it is not so trivial to realize $\delta_{\rm CP} \simeq 1.2$ [rad]. Note that in this pattern, the origin of the CP-violating phase is only a real part of the complex structure modulus parameter, i.e., $\mathrm{Re}\,\tau$ since all the SS phases are set to be zero. Figures 4 and 5 tell us that the quark flavor structure, i.e., the mass hierarchies and small mixing angles of the SM quarks, is quite dependent on the values of $\mathrm{Re}\,\tau$ as well as the values of $\mathrm{Im}\,\tau$. Thus, we cannot fit the CP-violating phase by scattering $\mathrm{Re}\,\tau$ and the mass hierarchies and mixing angles by scattering $\mathrm{Im}\,\tau$, independently, and hence we need comprehensive analyses for the quark flavor structures by means of all of scattered Higgs VEVs, $\mathrm{Re}\,\tau$ and $\mathrm{Im}\,\tau$.

We count the number of the configurations where values of the CP-violating phase are located in the quasi-realistic range,

$$0.8 \times 1.208 \le \delta_{\rm CP} \le 1.2 \times 1.208 \quad [\text{rad}], \qquad (4.8)$$
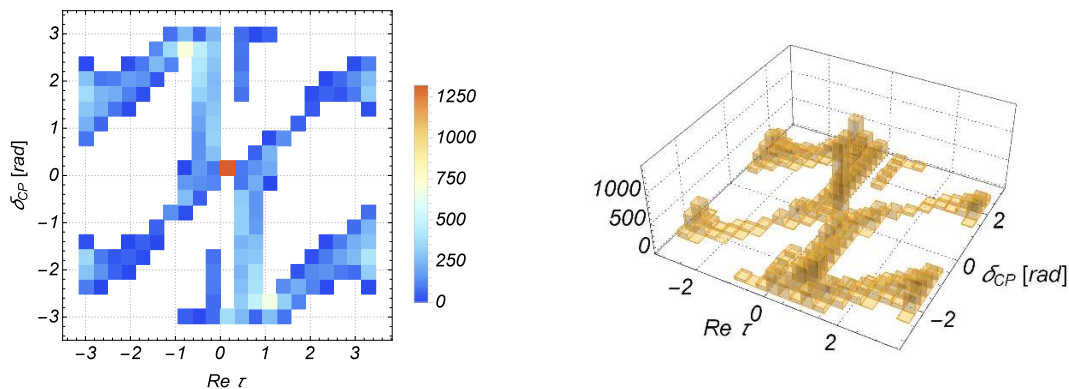
Figure 4. Distributions of the CP-violating phase δ_{CP} vs. real part of complex structure modulus $\mathrm{Re}\,\tau$ for $\mathrm{Im}\,\tau = 1.8$ in Pattern I.
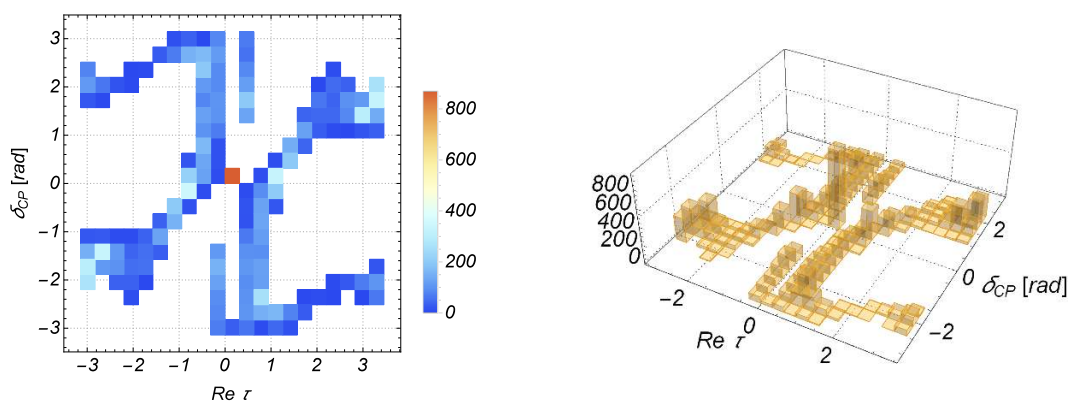
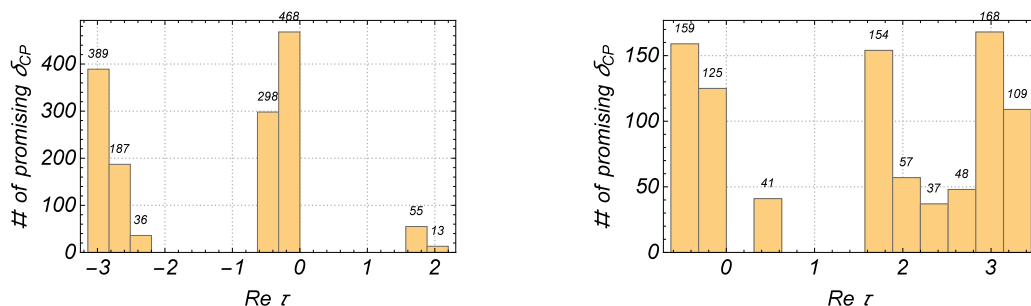

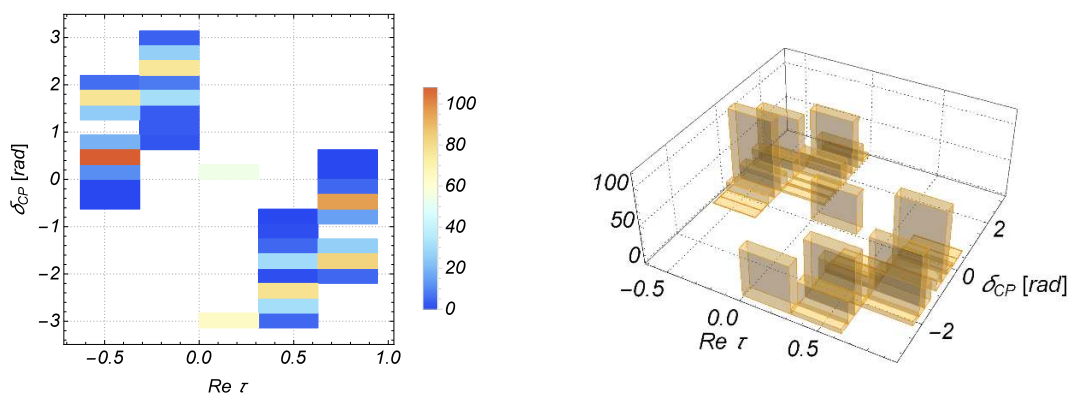**Figure 5**. Distributions of the CP-violating phase δ_{CP} vs. real part of complex structure modulus $\mathrm{Re}\,\tau$ for $\mathrm{Im}\,\tau = 2.0$ in Pattern I.

where we allow 20% deviations from the observed value shown in eq. (4.3). The distributions are as shown in figure 6, where various values of $\mathrm{Re}\,\tau$ result in realizing the observed quark profiles, including the CP phase δ_{CP} in Pattern I. In particular, we find characteristic peaks in the left and right panels of figure 6 around $\mathrm{Re}\,\tau \sim -3$ and -0.3 [for $\mathrm{Im}\,\tau = 1.8$] and $\mathrm{Re}\,\tau \sim -0.5, 1.5$ and 3 [for $\mathrm{Im}\,\tau = 2.0$], respectively. This difference between the positions of characteristic peaks also implies that an imaginary part of the complex structure modulus parameter affects the value of the CP-violating phase as well as the mass hierarchies of the quarks.

In addition to that, Pattern I and Pattern IV are more promising than the others in the point of how many configurations derive suitable δ_{CP} defined in eq. (4.8), as we will see later. This is easily found from the number of allowed configurations after the three cuts eqs. (4.5)–(4.7) and the region for δ_{CP} in eq. (4.8). The method and procedure to analyze the CP-violating phase are the same as those for the other patterns.

Numerical analysis in Pattern II. Results are shown in figures 7 (for $\mathrm{Im}\,\tau = 1.7$) and 8 (for $\mathrm{Im}\,\tau = 1.9$) and also 9 (histograms). Note that in this pattern, the origin of the CP-violating phase is not only the complex-valued Yukawa couplings including the
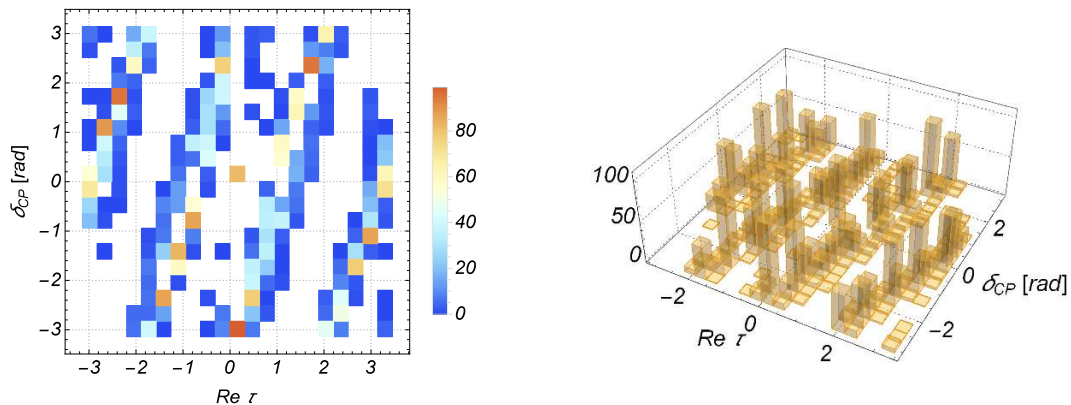
Figure 6. Left panel: frequency of $\mathrm{Re}\,\tau$ satisfying an inequality in eq. (4.8) for $\mathrm{Im}\,\tau = 1.8$ in Pattern I. Digits on the top of histogram bins denote the numbers of combinations of Higgs VEVs. Right panel: the same one for $\mathrm{Im}\,\tau = 2.0$.
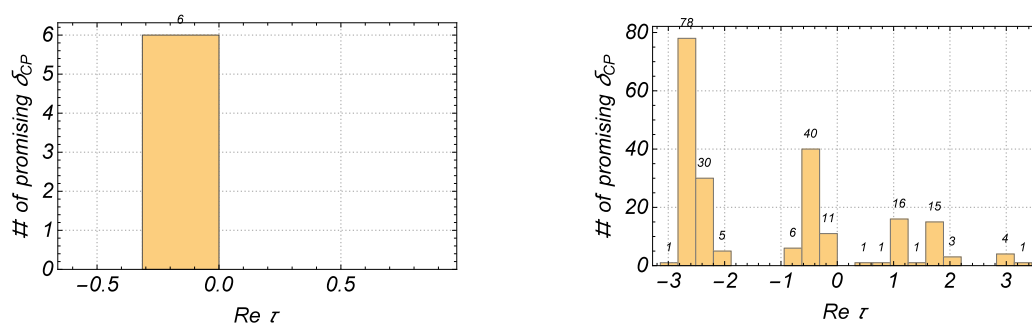

Figure 7. Distributions of the CP-violating phase δ_{CP} vs. real part of complex structure modulus $\mathrm{Re}\,\tau$ for $\mathrm{Im}\,\tau = 1.7$ in Pattern II.

product of the non-vanishing $\mathrm{Re}\,\tau$, but also "a" part in the definition of the Jacobi's theta function (2.5) due to nonzero SS phases. Figure 9 shows that to explain $\delta_{\mathrm{CP}} \simeq 1.2$ [rad], one needs $\mathrm{Re}\,\tau \sim -0.3$ for $\mathrm{Im}\tau = 1.7$ and the result is more determinative. On the other hand, figure 8 indicates that there exist various peaks in the right 3D histogram for $\mathrm{Im}\,\tau = 1.9$, and also that we cannot extract a characteristic prediction in this case. In addition, an conclusion revealed from figure 9 is that very limited points are only allowed by the numerical cuts.

Numerical analysis in Pattern III. Results are shown in figures 10 (for $\mathrm{Im}\,\tau = 1.9$), 11 (for $\mathrm{Im}\,\tau = 2.0$) and also 12 (histograms). Note that in this pattern, the origins of the CP-violating phase is the complex coefficient matrix (2.6) due to the SS phases, as well as the complex-valued Yukawa couplings including the non-vanishing $\mathrm{Re}\,\tau$ and "$c\nu$" part in the definition of the Jacobi's theta function (2.5). The case of $\mathrm{Im}\,\tau = 2.0$ is drastic, because it is impossible to simultaneously explain the quark flavor structure of mass hierarchies and mixing angles in this case.
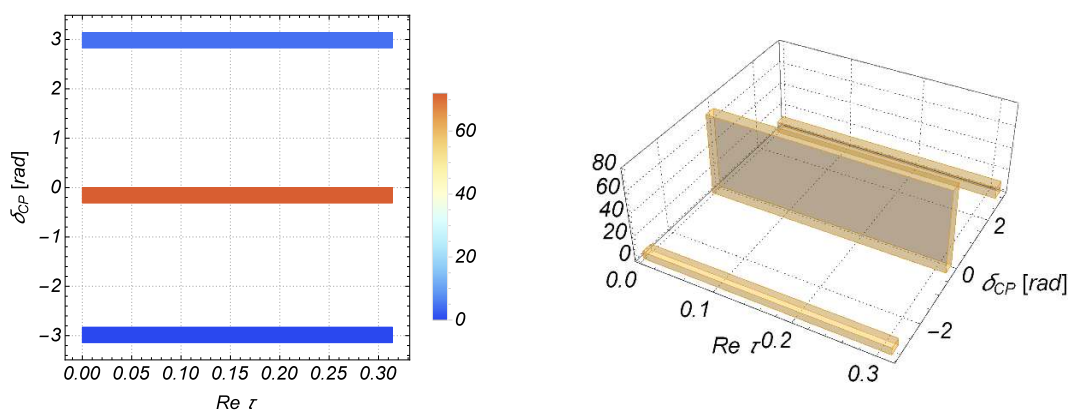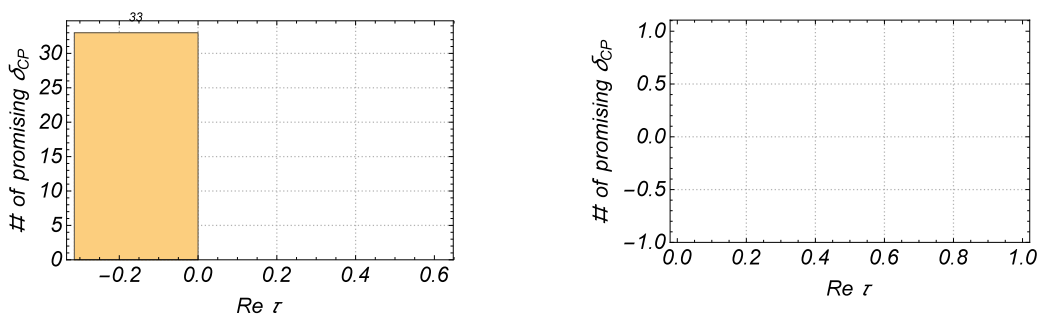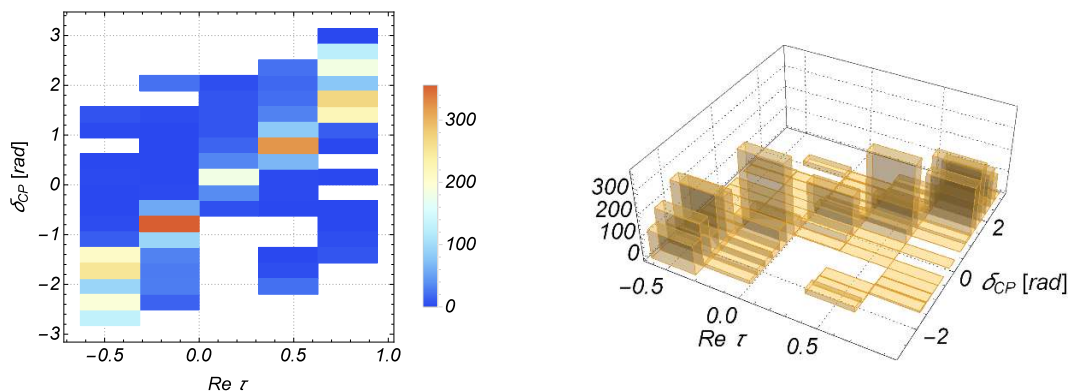
Figure 8. Distributions of the CP-violating phase $\delta_{\rm CP}$ vs. real part of complex structure modulus $\mathrm{Re}\,\tau$ for $\mathrm{Im}\,\tau = 1.9$ in Pattern Ⅱ.

Figure 9. Left panel: frequency of $\mathrm{Re}\,\tau$ satisfying an inequality in eq. (4.8) for $\mathrm{Im}\,\tau = 1.7$ in Pattern Ⅱ. Digits on the top of histogram bins denote the numbers of combinations of Higgs VEVs. Right panel: the same one for $\mathrm{Im}\,\tau = 1.9$.
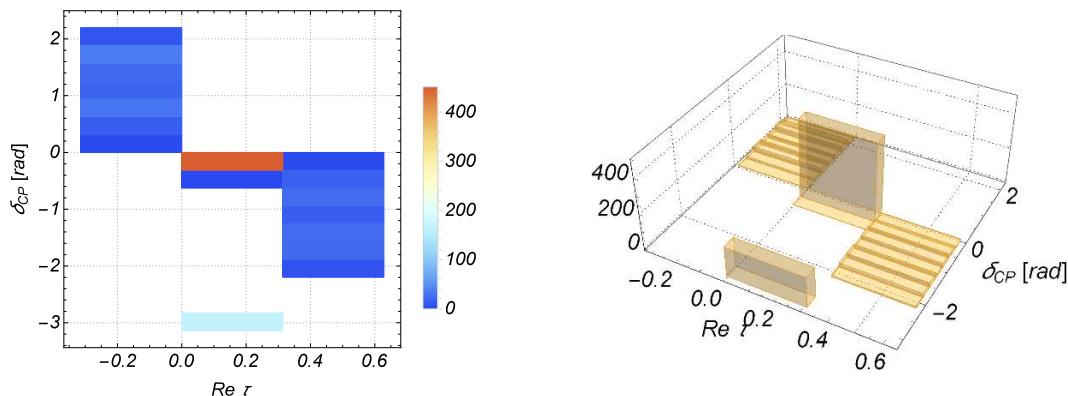
Figure 10. Distributions of the CP-violating phase δ_{CP} vs. real part of complex structure modulus $\mathrm{Re}\,\tau$ for $\mathrm{Im}\,\tau = 1.9$ in Pattern Ⅲ.

Figure 11. Distributions of the CP-violating phase δ_{CP} vs. real part of complex structure modulus $\mathrm{Re}\,\tau$ for $\mathrm{Im}\,\tau = 2.0$ in Pattern Ⅲ.

Figure 12. Left panel: frequency of $\mathrm{Re}\,\tau$ satisfying an inequality in eq. (4.8) for $\mathrm{Im}\,\tau = 1.9$ in Pattern Ⅲ. Digits on the top of histogram bins denote the numbers of combinations of Higgs VEVs. Right panel: the same one for $\mathrm{Im}\,\tau = 2.0$.

Numerical analysis in Pattern Ⅳ. Results are shown in figures 13 (for $\mathrm{Im}\,\tau = 1.7$) and 14 (for $\mathrm{Im}\,\tau = 1.9$) and also 15 (histograms). Note that in this pattern, similar to the previous Pattern Ⅲ, the origin of the CP-violating phase comes from both of the complex-valued Yukawa couplings with the non-vanishing $\mathrm{Re}\,\tau$ and the coefficient matrices of two
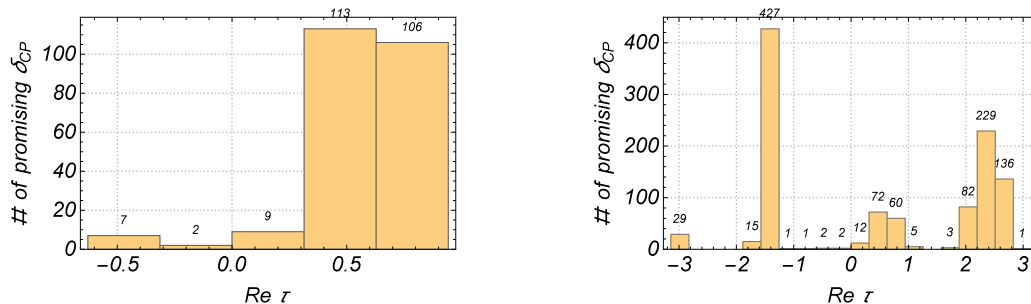
Figure 13. Distributions of the CP-violating phase δ_{CP} vs. real part of complex structure modulus $\text{Re}\,\tau$ for $\text{Im}\,\tau = 1.7$ in Pattern IV.

Figure 14. Distributions of the CP-violating phase δ_{CP} vs. real part of complex structure modulus $\text{Re}\,\tau$ for $\text{Im}\,\tau = 1.9$ in Pattern IV.

Figure 15. Left panel: frequency of $\text{Re}\,\tau$ satisfying an inequality in eq. (4.8) for $\text{Im}\,\tau = 1.7$ in Pattern IV. Digits on the top of histogram bins denote the numbers of combinations of Higgs VEVs. Right panel: the same one for $\text{Im}\,\tau = 1.9$.

sectors "1" and "2", i.e., $\mathcal{U}^{Z_2:\eta_X}$ ($X = 1, 2$). Figure 15 indicates that $\text{Re}\,\tau \sim 0.5$–0.75 can lead to the observed value of the CP-violating phase, $\delta_{CP} \simeq 1.2$ [rad], where the detail of a sample point is shown in table 3. On the other hand, the promising range of $\text{Re}\,\tau$ for $\text{Im}\,\tau = 1.9$ is around $\text{Re}\,\tau \sim -1.6$ and 2.2. This is easily understood also from the right panel in figure 14.

5 Conclusions and discussions

We have investigated properties of the CP-violating phase in the quark sector on toroidal orbifolds T^2/Z_N ($N = 2, 3, 4, 6$) with non-vanishing magnetic fluxes. In this system, a non-vanishing value is mandatory in the real part of the complex modulus parameter τ of the two torus in order to explain the CP violation in the quark sector. On T^2 without orbifolding, underlying discrete flavor symmetries severely restrict the form of Yukawa couplings and it is very difficult to reproduce the observed pattern in the quark sector including the CP-violating phase $\delta_{\rm CP}$. Only on the case of T^2/Z_2 orbifold with multiple Higgs doublets were focused, since under the other orbifoldings, i.e., T^2/Z_N ($N = 3, 4, 6$), the FN factor $e^{-{\rm Im}\,\tau}$ is not so small enough for causing the Gaussian FN mechanism. We numerically analyzed four patterns of the SS phases and as a result, it has been revealed that we can obtain realistic values near $\delta_{\rm CP} \sim 1.2$ [rad], by appropriate arrangement of the value of ${\rm Re}\,\tau$ for all of the patterns.

As concretely addressed in refs. [17, 40], in the present framework of the magnetized T^2/Z_2 orbifolds, multiple Higgs doublets are mandatory for realizing the observed quark masses and mixing angles. Here, let us comment on a possible problem via the existence of multiple Higgs doublets. In general, if no discrete symmetry or accidental cancellation realized by tuning of parameters happens, sizable tree-level flavor-changing neutral interactions are induced (in mass eigenbasis), which are highly disfavored by experimental results. To handle the danger without addressing symmetry or cancellation, except for the observed 125 GeV Higgs boson, doublet scalars are requested to be massive as much as around $10^2 \sim 10^3$ TeV. Dynamical realizations of Higgs μ terms with one light direction via D-brane instanton effects would give us an actual prescription (see e.g., [45, 46]).

A The other configuration of magnetic fluxes

The other samples of magnetic fluxes are shown in table 4. Here, three generations are realized in the quarks by taking $|M| = 6$, where nontrivial SS twists are mandatory, $\alpha \neq 0$ and/or $\beta \neq 0$ [14, 17]. Results of Pattern V are shown in figures 16, 17 and 18. We could not find realistic flavor structures in Pattern VI, where distributions of this pattern are not shown in the body. Figures 19, 20 and 21 contain the results of Pattern VII. Different from the configuration of M_X and η_X in eq. (4.2), the most disfavored pattern appears in the choice of the SS phases $\alpha_{1,2} = 1/2$, $\beta_{1,2} = 0$ (Pattern VI).
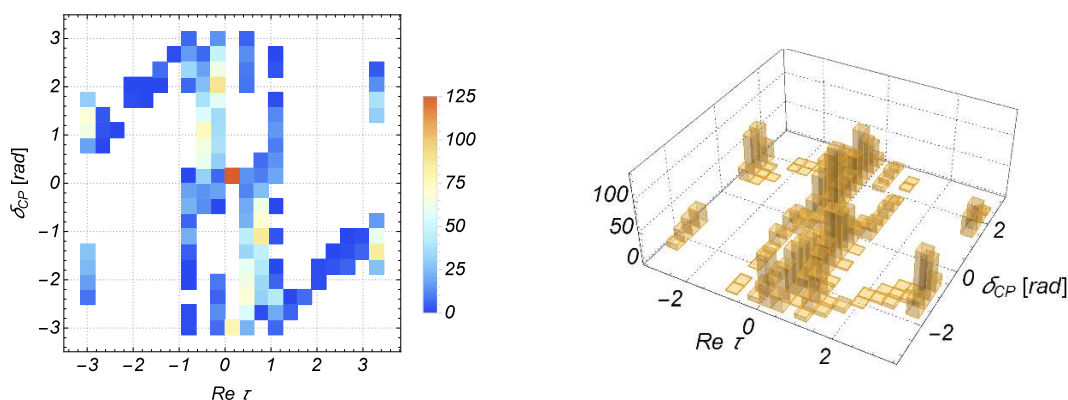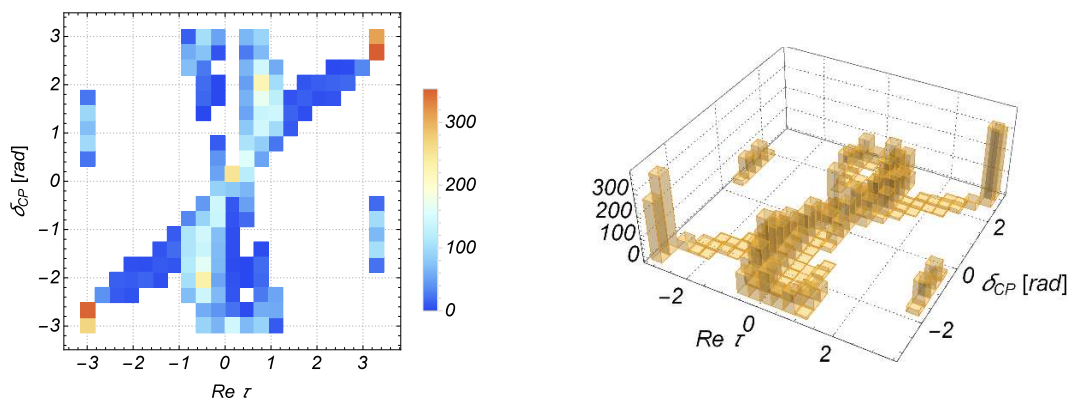
Figure 16. Distributions of CP-violating phase δ_{CP} vs. real part of complex structure modulus $\mathrm{Re}\,\tau$ for $\mathrm{Im}\,\tau = 1.8$ in Pattern V.
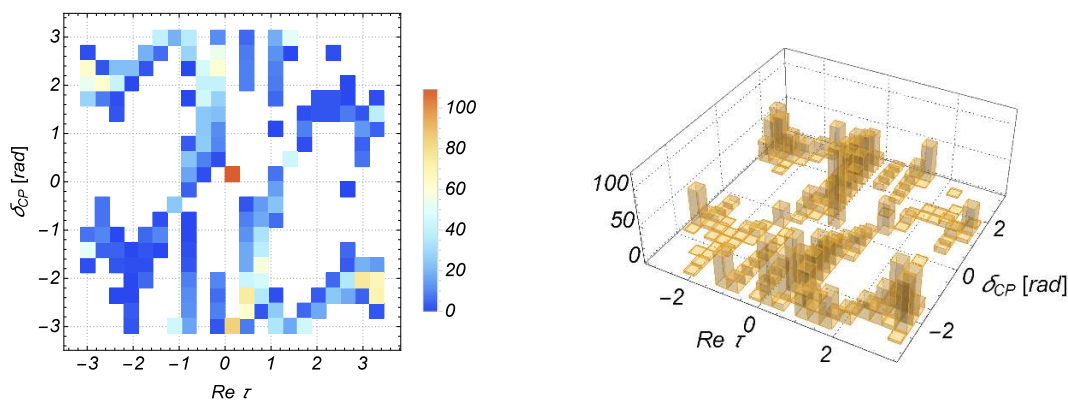
Figure 17. Distributions of CP-violating phase δ_{CP} vs. real part of complex structure modulus $\mathrm{Re}\,\tau$ for $\mathrm{Im}\,\tau = 2.0$ in Pattern V.
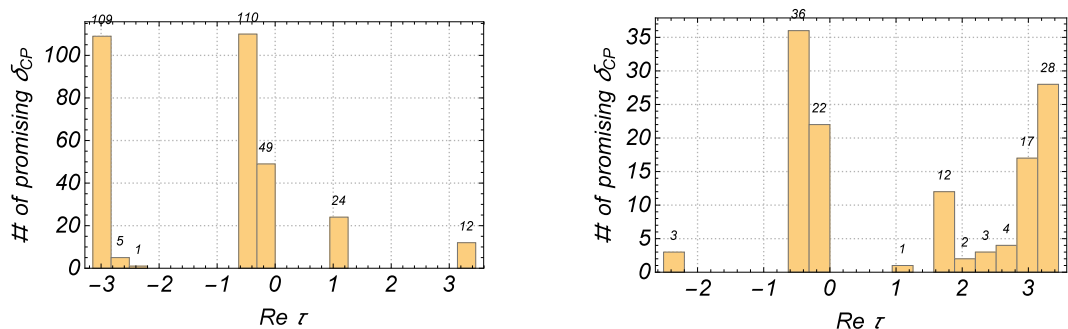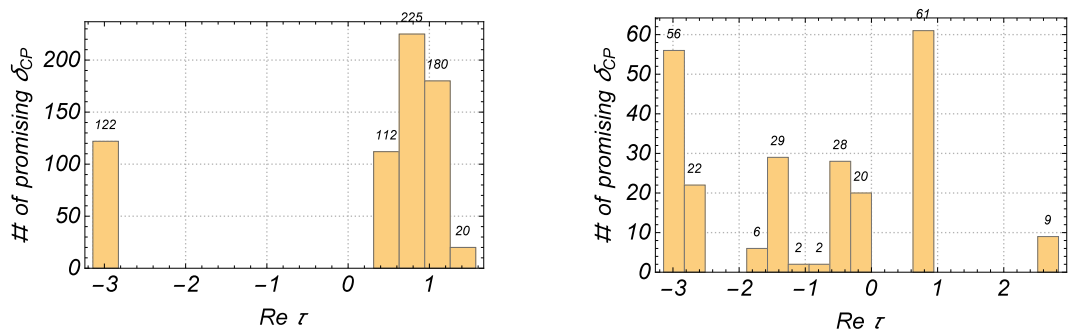

Figure 18. Left panel: frequency of $\mathrm{Re}\,\tau$ satisfying an inequality in eq. (4.8) for $\mathrm{Im}\,\tau = 1.8$ in Pattern V. Digits on the top of histogram bins denote the numbers of combinations of Higgs VEVs. Right panel: the same one for $\mathrm{Im}\,\tau = 2.0$.

Figure 19. Distributions of CP-violating phase δ_{CP} vs. real part of complex structure modulus $\mathrm{Re}\,\tau$ for $\mathrm{Im}\,\tau = 1.8$ in Pattern VII.
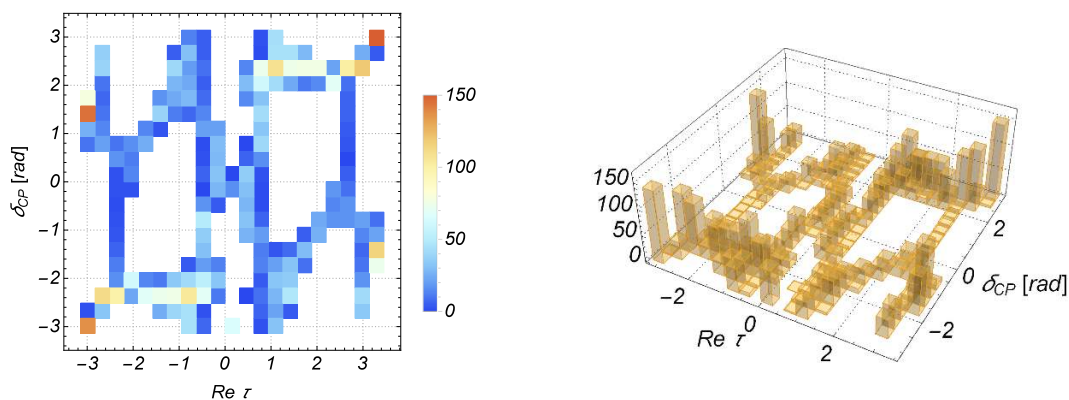
Figure 20. Distributions of CP-violating phase δ_{CP} vs. real part of complex structure modulus $\mathrm{Re}\,\tau$ for $\mathrm{Im}\,\tau = 2.0$ in Pattern VII.

Figure 21. Left panel: frequency of $\mathrm{Re}\,\tau$ satisfying an inequality in eq. (4.8) for $\mathrm{Im}\,\tau = 1.8$ in Pattern VII. Digits on the top of histogram bins denote the numbers of combinations of Higgs VEVs. Right panel: the same one for $\mathrm{Im}\,\tau = 2.0$.

	$\{M_1, \alpha_1, \beta_1, \eta_1\}$	$\{M_2, \alpha_2, \beta_2, \eta_2\}$	$\{M_3, \alpha_3, \beta_3, \eta_3\}$
Pattern V	$\{-6, 0, 1/2, +1\}$	$\{-6, 0, 1/2, -1\}$	$\{12, 0, 0, -1\}$
Pattern VI	$\{-6, 1/2, 0, +1\}$	$\{-6, 1/2, 0, -1\}$	$\{12, 0, 0, -1\}$
Pattern VII	$\{-6, 1/2, 1/2, +1\}$	$\{-6, 1/2, 1/2, -1\}$	$\{12, 0, 0, -1\}$

Table 4. The other samples of configurations.

References

[1] ATLAS collaboration, *Observation of a new particle in the search for the Standard Model Higgs boson with the ATLAS detector at the LHC*, *Phys. Lett.* **B 716** (2012) 1 [arXiv:1207.7214] [INSPIRE].

[2] CMS collaboration, *Observation of a new boson at a mass of* 125 *GeV with the CMS experiment at the LHC*, *Phys. Lett.* **B 716** (2012) 30 [arXiv:1207.7235] [INSPIRE].

[3] N. Arkani-Hamed, S. Dimopoulos and G.R. Dvali, *The hierarchy problem and new dimensions at a millimeter*, *Phys. Lett.* **B 429** (1998) 263 [hep-ph/9803315] [INSPIRE].

[4] I. Antoniadis, N. Arkani-Hamed, S. Dimopoulos and G.R. Dvali, *New dimensions at a millimeter to a Fermi and superstrings at a TeV*, *Phys. Lett.* **B 436** (1998) 257 [hep-ph/9804398] [INSPIRE].

[5] L. Randall and R. Sundrum, *A large mass hierarchy from a small extra dimension*, *Phys. Rev. Lett.* **83** (1999) 3370 [hep-ph/9905221] [INSPIRE].

[6] Y. Kawamura, *Triplet doublet splitting, proton stability and extra dimension*, *Prog. Theor. Phys.* **105** (2001) 999 [hep-ph/0012125] [INSPIRE].

[7] Y. Kawamura, *Split multiplets, coupling unification and extra dimension*, *Prog. Theor. Phys.* **105** (2001) 691 [hep-ph/0012352] [INSPIRE].

[8] N. Arkani-Hamed, S. Dimopoulos, G.R. Dvali and J. March-Russell, *Neutrino masses from large extra dimensions*, *Phys. Rev.* **D 65** (2001) 024032 [hep-ph/9811448] [INSPIRE].

[9] K. Agashe, G. Perez and A. Soni, *Flavor structure of warped extra dimension models*, *Phys. Rev.* **D 71** (2005) 016002 [hep-ph/0408134] [INSPIRE].

[10] G. Altarelli and F. Feruglio, *Tri-bimaximal neutrino mixing from discrete symmetry in extra dimensions*, *Nucl. Phys.* **B 720** (2005) 64 [hep-ph/0504165] [INSPIRE].

[11] D. Cremades, L.E. Ibáñez and F. Marchesano, *Computing Yukawa couplings from magnetized extra dimensions*, *JHEP* **05** (2004) 079 [hep-th/0404229] [INSPIRE].

[12] H. Abe, T. Kobayashi and H. Ohki, *Magnetized orbifold models*, *JHEP* **09** (2008) 043 [arXiv:0806.4748] [INSPIRE].

[13] Y. Fujimoto, T. Kobayashi, T. Miura, K. Nishiwaki and M. Sakamoto, *Shifted orbifold models with magnetic flux*, *Phys. Rev.* **D 87** (2013) 086001 [arXiv:1302.5768] [INSPIRE].

[14] T.-H. Abe, Y. Fujimoto, T. Kobayashi, T. Miura, K. Nishiwaki and M. Sakamoto, *Z_N twisted orbifold models with magnetic flux*, *JHEP* **01** (2014) 065 [arXiv:1309.4925] [INSPIRE].

[15] T.-H. Abe, Y. Fujimoto, T. Kobayashi, T. Miura, K. Nishiwaki and M. Sakamoto, *Operator analysis of physical states on magnetized T^2/Z_N orbifolds*, *Nucl. Phys.* **B 890** (2014) 442 [arXiv:1409.5421] [INSPIRE].

[16] H. Abe, K.-S. Choi, T. Kobayashi and H. Ohki, *Three generation magnetized orbifold models*, *Nucl. Phys.* **B 814** (2009) 265 [arXiv:0812.3534] [INSPIRE].

[17] T.-H. Abe et al., *Classification of three-generation models on magnetized orbifolds*, *Nucl. Phys.* **B 894** (2015) 374 [arXiv:1501.02787] [INSPIRE].

[18] H. Abe, T. Kobayashi, H. Ohki, A. Oikawa and K. Sumita, *Phenomenological aspects of 10D SYM theory with magnetized extra dimensions*, *Nucl. Phys.* **B 870** (2013) 30 [arXiv:1211.4317] [INSPIRE].

[19] H. Abe, T. Kobayashi, H. Ohki, K. Sumita and Y. Tatsuta, *Flavor landscape of 10D SYM theory with magnetized extra dimensions*, *JHEP* **04** (2014) 007 [arXiv:1307.1831] [INSPIRE].

[20] H. Abe, K.-S. Choi, T. Kobayashi and H. Ohki, *Non-Abelian discrete flavor symmetries from magnetized/intersecting brane models*, *Nucl. Phys.* **B 820** (2009) 317 [arXiv:0904.2631] [INSPIRE].

[21] H. Abe, K.-S. Choi, T. Kobayashi and H. Ohki, *Magnetic flux, Wilson line and orbifold*, *Phys. Rev.* **D 80** (2009) 126006 [arXiv:0907.5274] [INSPIRE].

[22] H. Abe, K.-S. Choi, T. Kobayashi, H. Ohki and M. Sakai, *Non-Abelian discrete flavor symmetries on orbifolds*, *Int. J. Mod. Phys.* **A 26** (2011) 4067 [arXiv:1009.5284] [INSPIRE].

[23] H. Abe, T. Kobayashi, H. Ohki, K. Sumita and Y. Tatsuta, *Non-Abelian discrete flavor symmetries of 10D SYM theory with magnetized extra dimensions*, *JHEP* **06** (2014) 017 [arXiv:1404.0137] [INSPIRE].

[24] H. Abe, T. Kobayashi, K. Sumita and Y. Tatsuta, *Gaussian Froggatt-Nielsen mechanism on magnetized orbifolds*, *Phys. Rev.* **D 90** (2014) 105006 [arXiv:1405.5012] [INSPIRE].

[25] H. Abe, J. Kawamura and K. Sumita, *The Higgs boson mass and SUSY spectra in 10D SYM theory with magnetized extra dimensions*, *Nucl. Phys.* **B 888** (2014) 194 [arXiv:1405.3754] [INSPIRE].

[26] H. Abe, K.-S. Choi, T. Kobayashi and H. Ohki, *Higher order couplings in magnetized brane models*, *JHEP* **06** (2009) 080 [arXiv:0903.3800] [INSPIRE].

[27] W. Buchmüller, M. Dierigl, F. Ruehle and J. Schweizer, *Chiral fermions and anomaly cancellation on orbifolds with Wilson lines and flux*, *Phys. Rev.* **D 92** (2015) 105031 [arXiv:1506.05771] [INSPIRE].

[28] H. Abe, T. Horie and K. Sumita, *Superfield description of $(4+2n)$-dimensional SYM theories and their mixtures on magnetized tori*, *Nucl. Phys.* **B 900** (2015) 331 [arXiv:1507.02425] [INSPIRE].

[29] W. Buchmüller, M. Dierigl, F. Ruehle and J. Schweizer, *Split symmetries*, *Phys. Lett.* **B 750** (2015) 615 [arXiv:1507.06819] [INSPIRE].

[30] W. Buchmüller, M. Dierigl, F. Ruehle and J. Schweizer, *De Sitter vacua from an anomalous gauge symmetry*, *Phys. Rev. Lett.* **116** (2016) 221303 [arXiv:1603.00654] [INSPIRE].

[31] W. Buchmüller, M. Dierigl, F. Ruehle and J. Schweizer, *De Sitter vacua and supersymmetry breaking in six-dimensional flux compactifications*, *Phys. Rev.* **D 94** (2016) 025025 [arXiv:1606.05653] [INSPIRE].

[32] M. Green, J. Schwarz and E. Witten, *Superstring theory: volume* 2, *loop amplitudes, anomalies and phenomenology*, Cambridge Monographs on Mathematical Physics, Cambridge University Press, Cambridge U.K., (1987) [INSPIRE].

[33] A. Strominger and E. Witten, *New manifolds for superstring compactification*, *Commun. Math. Phys.* **101** (1985) 341 [INSPIRE].

[34] M. Dine, R.G. Leigh and D.A. MacIntire, *Of CP and other gauge symmetries in string theory*, *Phys. Rev. Lett.* **69** (1992) 2030 [hep-th/9205011] [INSPIRE].

[35] K.-W. Choi, D.B. Kaplan and A.E. Nelson, *Is CP a gauge symmetry?*, *Nucl. Phys.* **B 391** (1993) 515 [hep-ph/9205202] [INSPIRE].

[36] C.S. Lim, *CP violation in higher dimensional theories*, *Phys. Lett.* **B 256** (1991) 233 [INSPIRE].

[37] T. Kobayashi and C.S. Lim, *CP in orbifold models*, *Phys. Lett.* **B 343** (1995) 122 [hep-th/9410023] [INSPIRE].

[38] C.S. Lim, N. Maru and K. Nishiwaki, *CP violation due to compactification*, *Phys. Rev.* **D 81** (2010) 076006 [arXiv:0910.2314] [INSPIRE].

[39] M. Kobayashi and T. Maskawa, *CP violation in the renormalizable theory of weak interaction*, *Prog. Theor. Phys.* **49** (1973) 652 [INSPIRE].

[40] Y. Fujimoto, T. Kobayashi, K. Nishiwaki, M. Sakamoto and Y. Tatsuta, *Comprehensive analysis of Yukawa hierarchies on T^2/Z_N with magnetic fluxes*, *Phys. Rev.* **D 94** (2016) 035031 [arXiv:1605.00140] [INSPIRE].

[41] C. Jarlskog, *Commutator of the quark mass matrices in the standard electroweak model and a measure of maximal CP-violation*, *Phys. Rev. Lett.* **55** (1985) 1039 [INSPIRE].

[42] C. Jarlskog, *A basis independent formulation of the connection between quark mass matrices, CP-violation and experiment*, *Z. Phys.* **C 29** (1985) 491 [INSPIRE].

[43] T. Kobayashi and O. Lebedev, *Heterotic string backgrounds and CP-violation*, *Phys. Lett.* **B 565** (2003) 193 [hep-th/0304212] [INSPIRE].

[44] UTFIT collaboration, M. Bona et al., *The* 2004 *UTfit collaboration report on the status of the unitarity triangle in the Standard Model*, *JHEP* **07** (2005) 028 [hep-ph/0501199] [INSPIRE].

[45] H. Abe, T. Kobayashi, Y. Tatsuta and S. Uemura, *D-brane instanton induced μ terms and their hierarchical structure*, *Phys. Rev.* **D 92** (2015) 026001 [arXiv:1502.03582] [INSPIRE].

[46] T. Kobayashi, Y. Tatsuta and S. Uemura, *Majorana neutrino mass structure induced by rigid instantons on toroidal orbifold*, *Phys. Rev.* **D 93** (2016) 065029 [arXiv:1511.09256] [INSPIRE].